

Binary logic operations with artificial molecular machines

Federico Nicoli^{a,b}, Erica Paltrinieri^{a,b}, Marina Tranfić Bakić^{a,b}, Massimo Baroncini^{a,c},
Serena Silvi^{a,d}, Alberto Credi^{a,b,*}

^a CLAN-Center for Light Activated Nanostructures, Institute for Organic Synthesis and Photoreactivity, Consiglio Nazionale delle Ricerche, via Gobetti 101, 40129 Bologna, Italy

^b Dipartimento di Chimica Industriale "Toso Montanari", Università di Bologna, viale del Risorgimento 4, 40136 Bologna, Italy

^c Dipartimento di Scienze e Tecnologie Agro-alimentari, Università di Bologna, viale Fanin 44, 40127 Bologna, Italy

^d Dipartimento di Chimica "G. Ciamician", Università di Bologna, via Selmi 2, 40126 Bologna, Italy

ARTICLE INFO

Article history:

Received 30 July 2020

Received in revised form 3 September 2020

Accepted 4 September 2020

Keywords:

Molecular shuttle

Nanoscience

Photochemistry

Rotaxane

Supramolecular chemistry

ABSTRACT

Living systems rely on ions and molecules for gathering, elaborating and storing information, as well as for controlling motion across different length scales. Artificial mimics of such biomolecular systems, i.e., logic devices and mechanical machines, have been developed in the past decades. Here we discuss their combination to produce logic-controlled nanomachines, a research that holds great potential for basic science and prospective applications. Systems of this kind may be forerunners of 'molecular robots' that can execute specific functions as a result of gathering and processing multiple environmental stimuli.

© 2020 Elsevier B.V. All rights reserved.

Contents

1. Introduction	1
2. Artificial molecular machines: a few basic concepts	2
3. Molecular logic gates and circuits	2
4. Combinational logic systems	3
5. Sequential logic systems	9
6. Conclusion	12
Declaration of Competing Interest	13
Acknowledgments	13
References	13

1. Introduction

Molecular machines are assemblies of molecular components that can exhibit mechanical movements in response to external

stimuli [1–4]. Nanoscale devices of this kind are present in all living organisms, where they are tasked with crucial functions such as intracellular transport, cell replication, process regulation and energy conversion [5]. It has been estimated that approximately ten thousand different types of molecular machines operate in the human body [6]. The ubiquitous presence of biomolecular machines and their important role in the natural world prove the utility and feasibility of nanotechnology [7,8], and motivate research on synthetic counterparts [9].

* Corresponding author at: CLAN-Center for Light Activated Nanostructures, Institute for Organic Synthesis and Photoreactivity, Consiglio Nazionale delle Ricerche, via Gobetti 101, 40129 Bologna, Italy.

E-mail address: alberto.credi@unibo.it (A. Credi).

In the past three decades, the progress in several areas of chemistry – in particular, supramolecular chemistry [10] – combined with the emergence of an engineering-type ingenuity [11], has enabled the design and realization of a large variety of artificial molecular devices and machines [1–3,12,13]. The field has now reached maturity [14], as also demonstrated by the award of the Nobel Prize in Chemistry 2016 to Jean-Pierre Sauvage [15], Fraser Stoddart [16] and Ben Feringa [17]. Synthetic molecular machines are expected to impel major progress in several areas of technology and medicine, and lead to applications – many of which are still unpredictable – in materials science, catalysis, energy conversion, information technology, drug delivery and medical therapies [18–21].

Artificial molecular machines are operated by chemical, electrochemical or photochemical inputs that provide the energy to activate the movements [22,23]. In the vast majority of the examples reported so far, the system responds to a single type of stimulus according to an on/off behavior. In fact, the operation of molecular machines as bistable mechanical switches can be interpreted in terms of binary (Boolean) logic [24], and it has been proposed that such devices could form the basis for future molecular-based binary memories [25]. Signal communication and transduction [26–28] can also be executed with synthetic molecular machines. On the other hand, biomolecular devices such as enzymes can be controlled by multiple signals according to complex patterns – a property that enables them to carry out sophisticated transformations with high control and fine regulation [6,29].

The analysis of the behavior of molecular species in terms of input-output flows by using the principles of Boolean algebra [30] opened the possibility of performing digital logic operations with molecules [1,23,31,32]. Since the first experimental demonstration of this concept [33], built upon the research performed on fluorescent chemosensors [34], many studies have highlighted the ability of molecular and supramolecular systems to process chemical or physical signals according to binary logic expressions [35–40]. Although the development of chemical devices that can outperform current silicon-based electronic computers is not around the corner, applications of molecular-based computation in the near future can be foreseen in combinatorial chemistry, intelligent materials, and medical diagnostics and therapy [31]. It is worth recalling that living organisms process, transfer and store information by means of molecular and ionic substrates under non-equilibrium conditions [6].

A key concept at the basis of both molecular-scale machines and logic devices is molecular switching [41], i.e., the reversible transformation of a molecule between (at least) two forms with different properties, triggered by external stimuli. Molecular switching has been widely investigated in solution and can also occur at interfaces, on surfaces and in the solid state. Thus, as it may be expected, the development of the field of stimuli-responsive nanoscale devices, such as mechanical machines and logic gates, has been closely related to the advances of research on molecular switches [42].

The combination of mechanical actuation and information processing, both performed at the nanometer scale using artificial molecular components, is indeed a fascinating yet sparsely investigated topic [43,44]. In this review, we describe examples of synthetic molecular machines that respond to more than one type of stimulus, and analyze the logic implications of their behavior. For clarity, they are categorized on the basis of the type of implemented digital logic. This kind of research addresses one of the most stimulating challenges in nanoscience – that is, the realization of intelligent systems and materials, capable of collecting and processing multiple inputs to perform useful tasks according to predetermined schemes.

2. Artificial molecular machines: a few basic concepts

Although the structure and/or shape of many chemical species can be modified by external stimuli, the term molecular machine

is referred to systems that exhibit large amplitude movements of their molecular components [3]. Artificial molecular machines can be assembled from different types of molecular and supramolecular systems, including nucleic acids [1–4]. Indeed, molecular machines cannot be considered as downsized versions of their macroscopic counterparts, because the behavior of nanometer-sized objects is quite different from that of macroscopic objects under several aspects. Thorough discussions on the operation mechanism of molecular machines, that is, how nanoscale entities can exploit an energy input to perform controlled movements in an environment dominated by random thermal motion, can be found elsewhere [4,7,9].

The majority of artificial molecular machines constructed until now are based on mechanically interlocked molecules, such as catenanes, rotaxanes and related species. Current synthetic methodologies and characterization techniques enable the preparation of this kind of compounds with high yields and the investigation of their structure and dynamic properties. The strategies that can be followed to construct and operate molecular machines based on mechanically interlocked species have been extensively described in several excellent books [1,12] and reviews [3,4,13,15,16].

Mechanically interlocked compounds are appealing for molecular machinery because: (i) the absence of strong chemical bonds between the molecular components allows them to perform rearrangements; (ii) the mechanical bond limits the amplitude of the intercomponent movements in three dimensions, and ensures the overall stability of the system; (iii) the population of a specific mutual arrangement of the components is determined by the strength of non-covalent interactions between them; and (iv) such interactions can be tuned by external inputs.

These features are briefly and nicely exemplified by rotaxanes (Fig. 1). They are composed, at minimum, of a macrocycle that encircles an axle-shaped molecule ([2]rotaxane); the presence of two bulky stoppers at the extremities of the axle prevents the disassembly of the components. Rotaxanes can undergo two interesting intercomponent rearrangements, namely, the translation (shuttling) of the ring along the axle (Fig. 1a), and the pirouetting of the ring around the axle (Fig. 1b). Systems of the first type, termed molecular shuttles, represent a widespread realization of the concept of molecular machine with synthetic molecules. In appropriately designed rotaxanes, these movements can be triggered by external stimuli; rotaxanes may thus be used to make both linear and rotary molecular machines.

In the past few decades, it has become evident that biomolecules such as nucleic acids and enzymes are useful building blocks to create nanoscale devices [29,45,46]. For example, molecular-level sensors, switches, machines and computing systems based on engineered DNA strands have been described [47,48]. The nearly unlimited possibilities offered by made-to-order nucleic acids in terms of structure and reactivity have enabled the realization of extremely sophisticated devices, such as rotary motors [49], programmable nanoscale assembly lines [50], logic-controlled interlocked DNA nanostructures [51], and responsive logic-gated allosteric devices [52] and nanorobots for targeted delivery [53,54]. A description of these artificial nanosystems, which are however built from naturally occurring molecules, is beyond the scope of this article and can be found elsewhere [1,4,6,55,56].

3. Molecular logic gates and circuits

Logic gates are devices that perform Boolean functions, i.e., binary operations on one or more inputs to produce an output [30]. Networks of logic gates connected to perform a more complex Boolean function form the basis of logic circuits. The specific pattern of

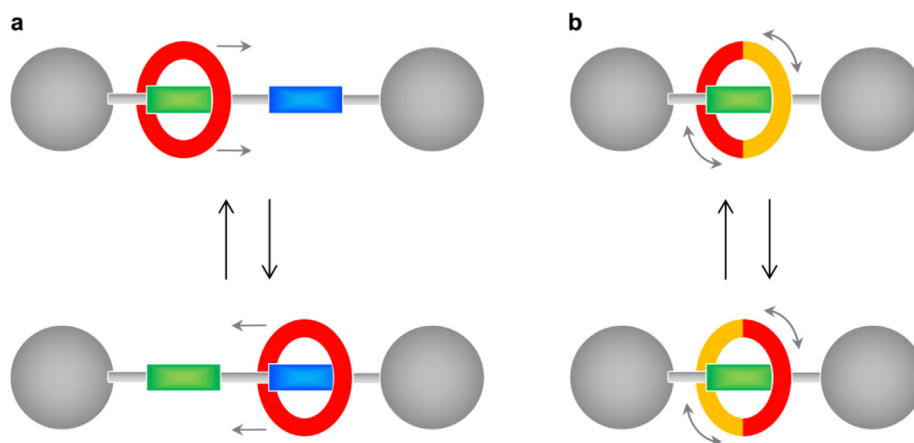


Fig. 1. Schematic representation of the principal intercomponent movements that can occur in a [2]rotaxane-based molecular machine: (a) ring shuttling, and (b) ring pirouetting.

input-output signals that characterize a logic gate or circuit is catalogued in the so-called *truth table*, that comprises all allowed combinations of input-output states. Obviously, the binary variables that define input and output states can assume only two values: 0 or 1. The semiconductor-based logic devices that populate our smartphones operate on electrical inputs and outputs. However, the concepts of binary logic are general and can thus be extended to any type of signal, including the physico-chemical ones present in the molecular world. The point is to design molecular-based devices that respond to such signals according to the desired logic rules. Although here we focus on Boolean logic, it should be recalled that, depending on the type of function that describes the physical input-output relationship (e.g. sigmoidal, exponential or linear), either discrete logic (binary or multi-valued) or infinite-valued (fuzzy) logic can be implemented [57].

Complex microelectronic circuits are constructed by interconnecting a large number of basic logic gates, each consisting of a few transistors [58]. Typically, the output of a given logic gate is fed as the input of the next gate (cascading). Such a connection, enabled by the homogeneity of the electrical input and output signals, is indeed a critical issue of molecular logic gates. The construction of molecular logic networks, however, can take advantage of functional integration achievable within one molecule by rational chemical design, rather than relying on extensive physical connection of elementary gates [31–40]. The ability of unsophisticated dye molecules to carry out complex logic functions in solution [59–61] which, in silicon-based systems, are performed by circuits made of several interconnected gates, demonstrates the feasibility of this approach.

Such a high functional integration arises from the possibility to reconfigure a molecular logic gate by changing the type of input-output signals or by using a separate switching stimulus. *Logic reconfiguration*, in fact, enables to define different operations for

the same gate and is an important property of molecular Boolean gates and circuits [31,62]. While in silicon-based circuits logic reconfiguration is usually achieved by the irreversible interruption of selected connections in gate arrays, molecular logic devices can be easily reconfigured, for instance, by monitoring the optical output signal at a different wavelength. In such systems, each selected output wavelength defines a different logic type. As multiple wavelengths can be monitored at the same time, these gates perform simultaneously different logic functions in response to a given set of inputs, a property called *superposition* or *multiplicity* of logic types [31,61]. Electronic systems cannot display such property, because it is a consequence of the multichannel nature of light. These concepts will be more clearly discussed with the aid of the examples presented in the next sections. They are divided into two categories, depending on whether their logic behavior is *combinational* (time independent) or *sequential* (time dependent) [63].

4. Combinational logic systems


In combinational logic, the output is determined only by the current state of the inputs [31,32,37–40,44]. The response of this kind of logic gates and circuits does not depend on time, because as soon as inputs are changed the information about the previous inputs is lost. The truth tables of most common two-input combinational logic gates, namely AND, OR, XOR and INH, are shown in Fig. 2. In a two-input AND gate the output is 1 only if both inputs are 1 (logic product); conversely, in a two-input OR gate it is sufficient that either input is 1 to have output 1 (logic sum). NAND (NOT AND) and NOR (NOT OR) gates, in which the output state is inverted with respect to AND and OR gates, respectively, are also very common. The XOR (eXclusive OR) gate has output 0 when both inputs are equal, i.e. they are both 0 or 1, and it has output 1 when exclusively one of the two inputs is 1. The INH (inhibit)

AND




In ₁	In ₂	Out
0	0	0
0	1	0
1	0	0
1	1	1

OR




In ₁	In ₂	Out
0	0	0
0	1	1
1	0	1
1	1	1

XOR



In ₁	In ₂	Out
0	0	0
0	1	1
1	0	1
1	1	0

INH



In ₁	In ₂	Out
0	0	0
0	1	0
1	0	1
1	1	0

Fig. 2. Truth table and conventional symbol of common two-inputs combinational logic operations.

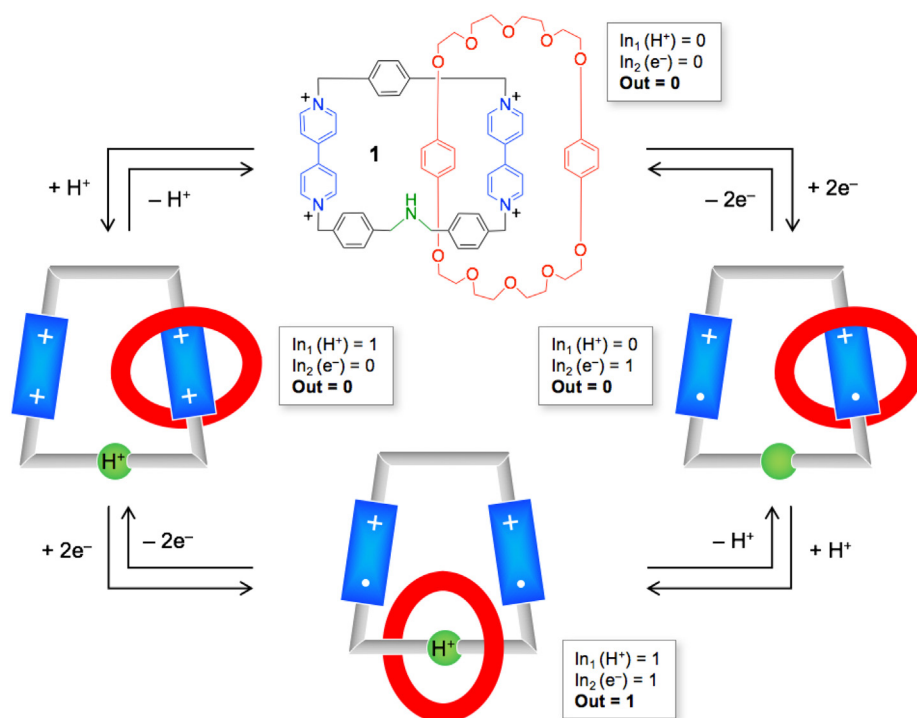


Fig. 3. Switching processes that occur in catenane **1** in solution. The position of the crown ether ring can be changed under acid/base and red/ox inputs according to AND logic [64].

operation is significant because it exhibits noncommutative behavior – that is, the output state is affected by exchanging the input states. In particular, the whole system is gated by one of the inputs; as shown in Fig. 2, when In_2 is 1 the output state is 0 regardless of the state of In_1 .

It has been observed that molecular switches operating under thermodynamic control can be related to combinational logic gates or circuits [44,62]. These devices combine the current input states (i.e., the set of conditions applied to the molecular switch) to yield the output (i.e., the state of the switch). In fact, the application of an input stimulus can bring the switch into a new equilibrium state; the starting equilibrium condition, however, will be immediately restored as soon as the perturbing stimulus is removed. Most artificial molecular machines reported so far follow such a behavior, as they are two-state, one-input thermodynamic switches [1,3,4]. This discussion can be easily extended to switches that can be interconverted between more than two states (multistable) and/or respond to more than one input (multifunctional) [1,41].

As discussed in Section 2, the components of mechanically interlocked molecules can be set in motion upon application of a physical or chemical stimulus. This paradigm has been widely implemented experimentally, allowing the construction of several kinds of artificial molecular machines [1–4,12,13]. Systems in which the movements are controlled by combinations of two inputs, however, are less frequent in the literature. An example is represented by the [2]catenane **1** (Fig. 3), consisting of an electron-rich aromatic crown ether interlocked with a cyclophane ring endowed with two electron-poor bipyridinium recognition sites [64]. The cyclophane also contains a secondary amine moiety, which can be easily converted into an ammonium center that can also function as a recognition site for the crown ether. Spectroscopic and electrochemical experiments showed that the crown ether encircles a bipyridinium unit of the other ring, irrespective of the protonation state of the amine site. In the protonated catenane, however, one-electron reduction of both the bipyridinium

units of **1** causes the movement of the crown ether onto the ammonium center. Hence, in order to switch the position of the crown ether ring (output), both the protonation of the amine center (input 1) and the reduction of the bipyridinium units (input 2) need to be performed. In other words, the mechanical motion in catenane **1** is controlled by acid/base and red/ox stimuli according to AND logic.

A semi-biological molecular machine capable of controlling the folding of a protein in response to adenosine triphosphate (ATP) and light inputs with AND logic was also described [65]. As shown schematically in Fig. 4, a genetically engineered chaperonin (GroEL) was functionalized at both entrance sides of its cylindrical cavity with azobenzene photoswitches. Azobenzene can exist in two configurations – the linear and apolar *trans*, and the bent and polar *cis* – that can be interconverted by light irradiation. GroEL, owing to hydrophobic interactions, can trap denatured green fluorescent protein (GFP) and prevent its refolding. Upon addition of ATP, the chaperonin assumes an open arrangement, so that GFP is released from the cavity and can adopt its folded conformation. The release of GFP, however, is considerably faster when the *trans*-azobenzene gates are converted to the *cis*-isomer by UV light irradiation, most likely as a result of the lower hydrophobicity of *cis*-azobenzene compared with the *trans* isomer. Conversely, slow or no refolding of the denatured GFP was observed upon stimulation with either ATP or UV light. Thus, the release and subsequent folding of the protein takes place efficiently only when both ATP and light inputs are supplied (Fig. 4). From a general perspective, molecular machines that perform a biologically relevant action in response to a set of environmental stimuli following a predetermined logic function could represent a first step forward towards nanodevices capable of autonomously diagnosing diseases and effecting therapies [31,66].

A chemical ensemble that combines a logic gate and a molecular machine was described very recently [67]. The design exploits the ionic output of an AND operation, performed on two ionic

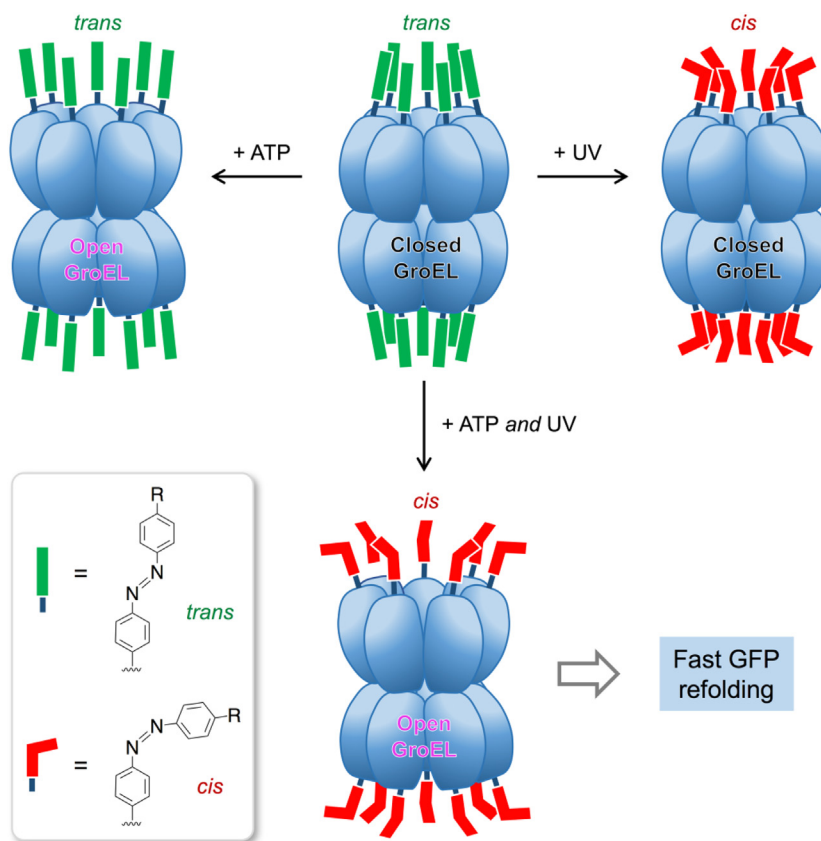


Fig. 4. An azobenzene-modified GroEL chaperonin can control the refolding of denatured green fluorescent protein (GFP) in response to chemical (ATP) and light (UV) stimulation according to AND logic [65].

inputs, to activate a molecular rotor which, in its turn, acts as a catalyst for a click reaction. The components of the logic gate are the bis-chelating species **2** and **3**, which contain bidentate 1,10-phenanthroline (PHEN)-type and tridentate 2,2':6',2''-terpyridine (TPY)-type ligands (Fig. 5a). The components of the molecular machine are stator **4**, rotor **5** and pivot **6** (Fig. 5b). The operation of the ensemble in CH_2Cl_2 - CH_3CN 15:1 is summarized in Fig. 6. The AND gate is based on an equimolar mixture of ligands **2** and **3**, and of Cu^+ ions; the input signals are encoded by the presence of Zn^{2+} and Hg^{2+} ions, while the output is represented by uncomplexed Cu^+ ions. In the initial state ($\text{In}_1 = \text{In}_2 = 0$) the copper ions are complexed by **2** ($\text{Out} = 0$) because of the higher affinity of the chelating site of **2** with respect to **3**. The addition of a stoichiometric amount of Zn^{2+} ions ($\text{In}_1 = 1$, $\text{In}_2 = 0$) causes the formation of the zinc complex of **2** and the translocation of Cu^+ to ligand **3** ($\text{Out} = 0$). The subsequent addition of 1 equivalent of Hg^{2+} ions ($\text{In}_1 = \text{In}_2 = 1$) displaces Cu^+ from **3**, thus releasing the former in the solution ($\text{Out} = 1$). If Hg^{2+} ions are added first ($\text{In}_1 = 0$, $\text{In}_2 = 1$), the mercury complex of **3** is formed, without affecting the copper complex of **2** ($\text{Out} = 0$); the subsequently added Zn^{2+} ($\text{In}_1 = 1$, $\text{In}_2 = 1$) eventually displaces Cu^+ from **2**, thus generating the chemical output.

In the presence of two Cu^+ ions, stator **4**, rotor **5** and pivot **6** self-assemble to yield a molecular rotor that exhibits a catalytic activity (Fig. 6) [68]. Thus, the previously discussed AND gate, which furnishes Cu^+ ions as the output, could be used to assemble the molecular machine in response to Zn^{2+} and Hg^{2+} inputs. This possibility was investigated by NMR spectroscopy on a solution containing

$\text{Cu}(\text{CH}_3\text{CN})_4^+$, **2**, **3**, **4**, **5** and **6** in a 2:2:2:1:1:1 ratio. The experiments showed that the molecular rotor is formed upon addition of both Zn^{2+} and Hg^{2+} inputs, and that it catalyzes (at 1 mol %) the cycloaddition between alkyne **7** and azide **8** (Fig. 6). The ensemble, whose main drawback is the long response time (the Zn^{2+} -induced translocation of Cu^+ from **2** to **3** takes three hours at room temperature), could be reset by removing zinc and mercury ions using hexacyclen as a competitive host. Overall, three reactive systems – logic gate, molecular rotor and alkyne-azide pair – are operated in a cascade and communicate together by means of ionic signals. This remarkable result highlights the power of supramolecular chemistry to devise synthetic mechanical nanodevices that can perform functions under the control of a specific matrix of chemical effectors. Research along this line can also contribute to understanding (and, one day, mimicking) the pathways that underlie signaling, regulation and activity in complex biological ensembles [7].

Another interesting case of AND logic involving molecular machines is represented by functionalized mesoporous silica nanoparticles [69]. It was shown previously that the uptake and release of guest molecules from the nanopores of such particles can be controlled by surface-attached rotaxane-type molecular machines activated by external stimuli [70]. In fact, the ring component of the rotaxane, by shuttling along the axle towards the mesoporous silica surface or away from it, prevents or allows the transit of the molecular guests through the pores, thereby acting as 'nanovalves'. On the other hand, it was observed that guest release from the nanoparticles could also be photoinduced by

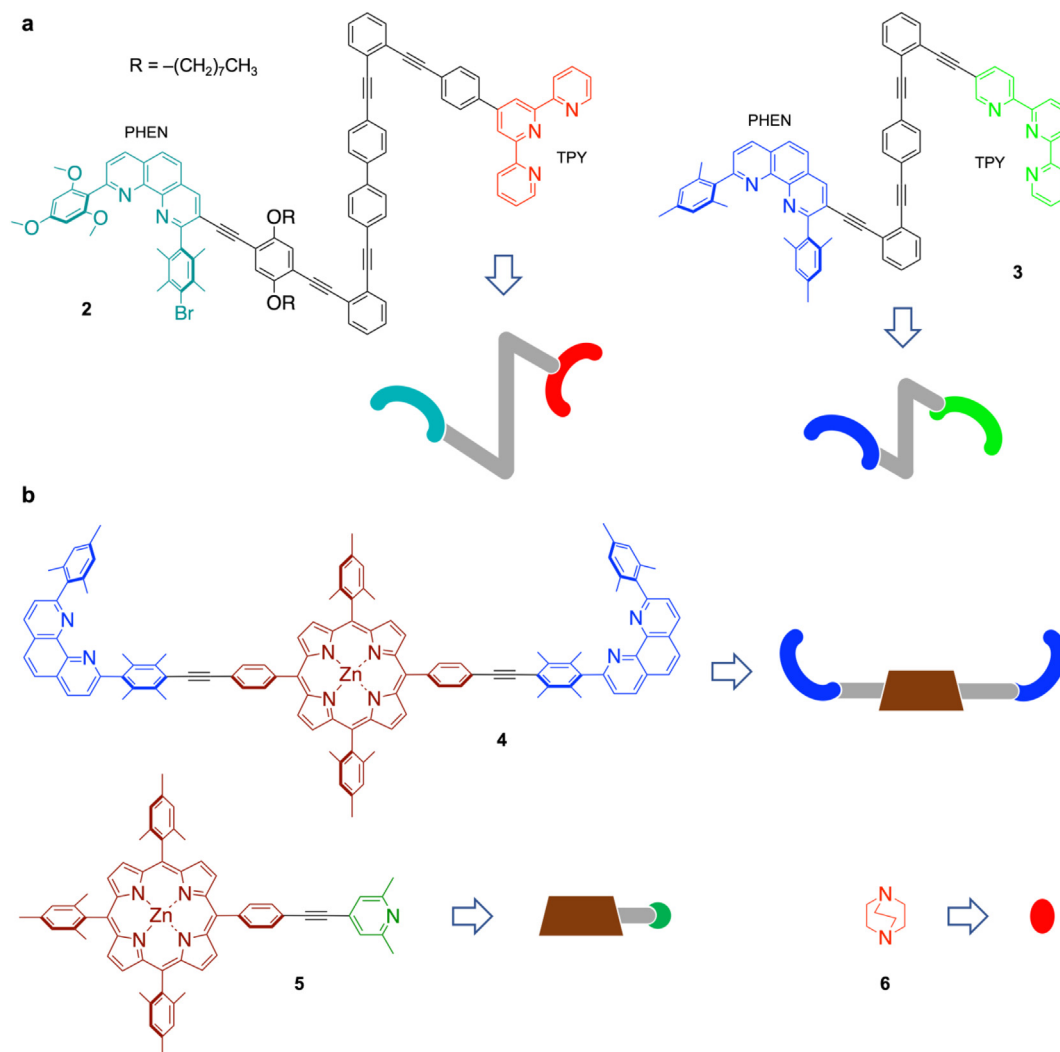


Fig. 5. Structure formulas and schematic representation of: (a) compounds **2** and **3**, utilized to perform an AND logic operation with Zn²⁺ and Hg²⁺ as the inputs and Cu⁺ as the output; (b) stator **4**, rotor **5** and pivot **6**, that self-assemble into a molecular rotor in the presence of Cu⁺ ions [67].

functionalizing the interior of the nanopores with molecular photoswitches such as, for example, azobenzene units [71]. It was proposed that the wagging motion associated with dynamic *trans-cis* isomerization when azobenzene derivatives are irradiated with a wavelength of light absorbed by both the *trans* and *cis* isomers can impel guest molecules out of the nanopores. The novel dual-controlled nanoparticles include both pH-responsive nanovalves and photoresponsive azobenzene nanoimpellers, such that the efficient release of encapsulated guest molecules (output) is obtained by activating both the nanovalves (with pH changes; input 1) and the nanoimpellers (with blue light; input 2) [70]. In view of drug delivery applications, logic activation is promising for achieving a superior level of controlled release with respect to common switches. Furthermore, if one input is endogenous (e.g., a pH change) and the other is external (e.g., light), it might be possible to combine autonomous and manual release mechanisms to fine-tune the dosage delivered to a specific tissue or region.

A rotaxane that exhibits a INH response to red/ox and acid/base stimulation is represented in Fig. 7a [72]. Compound **9** is a [1]rotaxane, i.e., a species wherein a molecular axle is threaded into a macrocycle to which it is also covalently connected [73]. The rotaxane contains a ferrocene unit (Fc), whose upper and lower cyclopentadienyl rings are respectively linked to a crown ether and to an axle that comprises a dibenzylammonium (DBA) and

methyltriazolium (MT) recognition sites, stoppered by a fluorescent naphthalimide moiety (NI). In this system the chemical input signals are represented by a base (1,8-diazabicyclo[5.4.0]undec-7-ene) capable of switching off the DBA site by deprotonation, and an oxidant [Fe(ClO₄)₃] capable of oxidizing ferrocene to its monocationic form (Fc⁺); the output signal is encoded by the relative change of the NI-based fluorescence with respect to the initial state [$\Delta F = (F_0 - F)/F_0$] (Fig. 7b). As shown in Fig. 7c, in the absence of any input the NI-based fluorescence band is evident (In₁ = 0, In₂ = 0, Out = 0). If, however, two equivalents of base are added, the emission intensity is significantly decreased ($\Delta F > 80\%$), most likely because the NI-based excited state is quenched by an electron-transfer process from the electron-rich Fc unit (In₁ = 1, In₂ = 0, Out = 1). The ¹H NMR spectra show that the macrocyclic ring initially encircles the DBA site, and moves towards the MT site when the former is deprotonated by the base. In the initial state, wherein the Fc unit is kept far away from NI owing to the interaction between the macrocycle and the DBA site, such a quenching process is inefficient. The original intensity is fully recovered upon addition of acid. Hence, the acid/base-induced distance change between Fc and NI in rotaxane **9** is transduced into a luminescence variation. Interestingly, such a switching phenomenon is jeopardized by oxidation of Fc to Fc⁺ by means of Fe(III) perchlorate (Fig. 7d). The NI-based fluorescence intensity of the oxidized rotax-

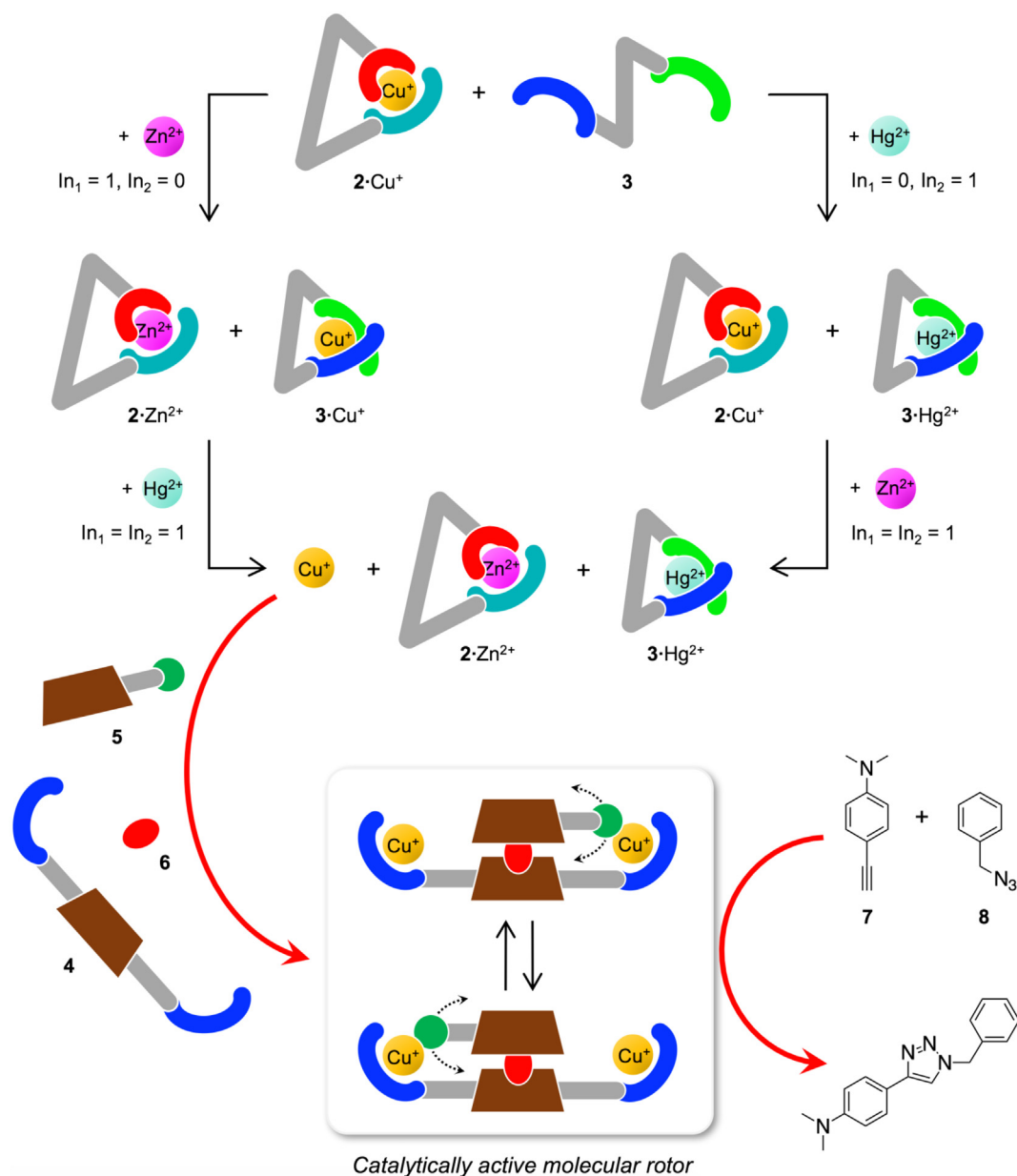


Fig. 6. Operation scheme of an AND logic-controlled catalytic nanorotor based on coordination compounds [67]. The structural formulas of the molecular components are shown in Fig. 5. The red arrows highlight the cascading of the three reactive systems: logic gate, molecular machine and cycloaddition precursors. (For interpretation of the references to colour in this figure legend, the reader is referred to the web version of this article.)

ane is similar to that of the non-oxidized one ($\Delta F < 10\%$) and is unaffected by the acid/base input ($\text{In}_1 = 0$ or 1 , $\text{In}_2 = 1$, $\text{Out} = 0$). Thus, the binary logic behavior of the fluorescence of **9** in response to acid/base and red/ox inputs corresponds to the INH gate (Fig. 7b) in which the gating input is the red/ox one (In_2).

A peptide-based [2]rotaxane was found to exhibit fluorescence changes, upon addition of acid and dimethylsulfoxide (DMSO) solvent, that correspond to the INH function [74]. The logic behavior was also observed in patterned polymer films containing the rotaxane, when exposed to trifluoroacetic acid and DMSO vapors, although the chemical reset after the activation of the acid input (that is, neutralization) caused a deterioration of the optical quality of the film.

The first example of a molecular XOR gate was based on the chemically triggered threading and dethreading of macrocyclic and acyclic molecular components in solution [75]. This work

received considerable attention [76] because: (i) studies on the stimuli-controlled assembly and disassembly of pseudorotaxanes have been instrumental for the development of more sophisticated molecular machines based on rotaxanes and catenanes [1,3], and; (ii) the XOR function can be utilized to compare the digital state of two signals, and it is a key component of half-adder and half-subtractor circuits at the basis of binary sum and difference [30]. Recent more detailed investigations on the UV-visible spectroscopic properties of this system in response to acid/base stimulation revealed that it can also operate as a bidirectional half subtractor with logic reversibility [77].

In organic solution, the electron-rich macrocycle **10** and electron-poor 2,7-diazapyrenium axle-like derivative **11** self-assemble to yield a pseudorotaxane (Fig. 8a), stabilized by charge-transfer (CT) interactions. The separated ring and axle components show strong and structured absorption bands, and an

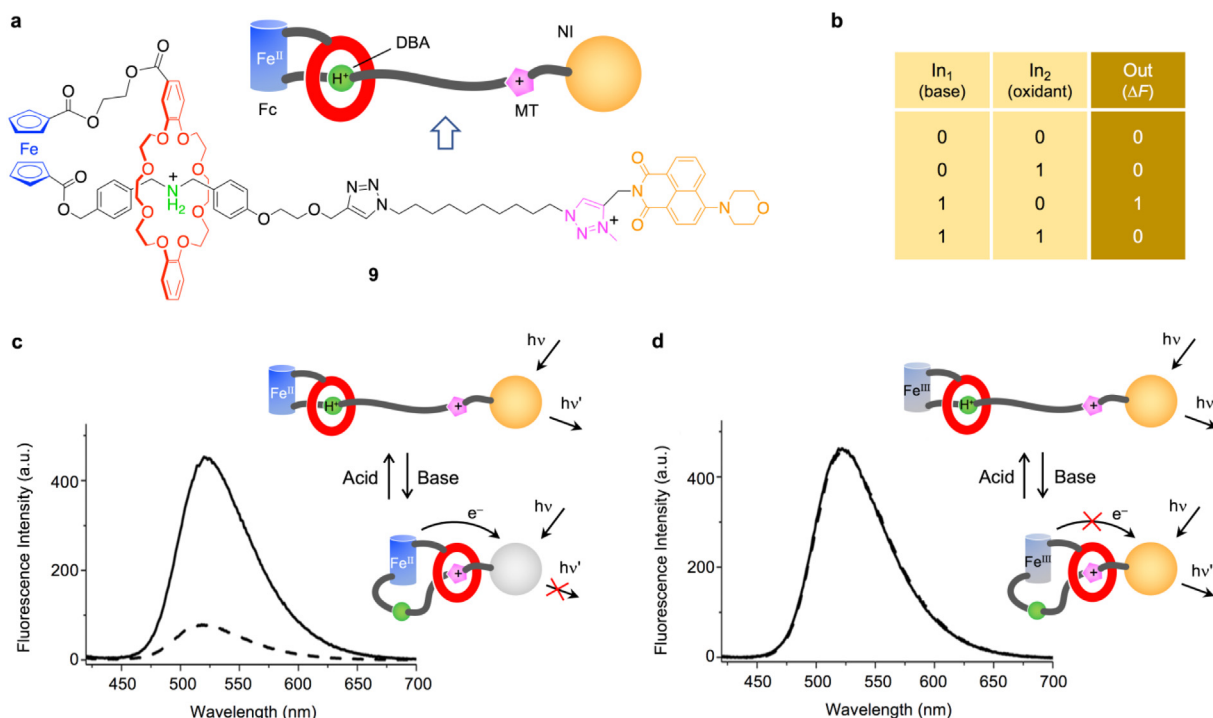


Fig. 7. (a) Structural formula and schematic representation of [1]rotaxane **9**. (b) Truth table showing the INH-type fluorescence response of **9** to acid/base and red/ox inputs. (c) Emission spectra of **9** showing the NI-based fluorescence band before (full line) and after (dashed line) the addition of 2.0 equivalents of the base 1,8-diazabicyclo[5.4.0]undec-7-ene. (d) Emission spectra of **9**, treated with 5.0 equivalent of the oxidant $\text{Fe}(\text{ClO}_4)_3$, before (full line) and after (dashed line) the addition of 2.0 equivalents of base. The switching mechanism is depicted in the insets. Conditions: CH_2Cl_2 , $\lambda_{\text{ex}} = 409 \text{ nm}$. Adapted by permission from Ref. [72], Copyright 2013 American Chemical Society.

intense fluorescence (Fig. 9). Complexation is revealed by as many as three different optical signals: (i) the appearance of a yellow colour because of the presence of a CT absorption tail in the visible region, (ii) the quenching of the UV fluorescence of **10** ($\lambda_{\text{max}} = 340 \text{ nm}$), and (iii) the quenching of the blue-green fluorescence of **11** ($\lambda_{\text{max}} = 428 \text{ nm}$).

In all cases, the inputs of this system are activated by the addition of sufficient amounts (30 equivalents) of an aliphatic amine (tributylamine, TBA; In_1) and acid ($\text{CF}_3\text{SO}_3\text{H}$; In_2). For the XOR function, the output state is encoded by the fluorescence intensity of **10** at 340 nm (Out_1). The operation mechanism of the device is illustrated schematically in Fig. 8b and 9b. As mentioned above, when the two inputs are not present the fluorescence of **10** is quenched in the pseudorotaxane ($In_1 = In_2 = 0$, $\text{Out}_1 = 0$). When only the amine input is applied, the complex dethreads because a stronger CT interaction between TBA and **11** is formed. Under such conditions, the fluorescence of free **10** is not quenched ($In_1 = 1$, $In_2 = 0$, $\text{Out}_1 = 1$). The fluorescence typical of free **11** at 428 nm is still quenched, and a new luminescence band at 666 nm, deriving from the complex between **11** and TBA, is observed. On the other hand, the application of the acid input alone causes the protonation of **10** and, again, dethreading of the pseudorotaxane and revival of the fluorescence of free **11**. As the protonated form of **10** has the same emission properties of the neutral form, the output at 340 nm is switched to state 1 upon activation of the H^+ input ($In_1 = 0$, $In_2 = 1$, $\text{Out}_1 = 1$). When both inputs are applied, the acid and the base mutually annihilate, the complex remains associated and the emission intensity at 340 nm is quenched ($In_1 = 1$, $In_2 = 1$, $\text{Out}_1 = 0$). Hence, the output logic state can be 1 only if *exclusively one* of the two inputs is activated, as foreseen for XOR logic (Figs. 2 and 9b).

Interestingly, wavelength reconfiguration of the luminescence readout affords double inhibit (INH) behavior (Fig. 9). If the output is monitored at 428 nm (fluorescence of free **11**; Out_2) or at 666 nm

(fluorescence of the CT complex between **11** and TBA; Out_3), the system behaves as an INH gate with TBA (In_1) or H^+ (In_2) as the gating inputs, respectively. The superposition of the XOR and two complementary INH gates enables to mimic the function of a bidirectional half subtractor. In other words, this logic feature corresponds to the physical inversion of the input channels that represent the minuend and the subtrahend data in a conventional half subtractor, thus enabling the Boolean subtraction of two one-bit digits, A and B , in either order ($A - B$ and $B - A$). It should be noted that this supramolecular switch displays such advanced Boolean functionalities because of the high degree of logic integration, which originates from the peculiar and uncommon physico-chemical properties of the system. From another perspective, the relative molecular movements of the ring and the axle are controlled by a non-trivial combination of two simple chemical inputs.

The truth table displayed in Fig. 9b shows that two different input combinations, namely $In_1 = In_2 = 0$ and $In_1 = In_2 = 1$, produce the same set of output states, namely $\text{Out}_1 = \text{Out}_2 = \text{Out}_3 = 0$. Hence, the output state does not identify anymore a distinct input string, thus determining a loss of information upon performing the operation. Logic devices that erase information in their operation are said to be *irreversible*. Landauer showed that irreversible logic computations, which are commonplace for molecular logic gates and circuits, produce an increase of the entropic content of the system, thus dissipating an amount of heat energy equal to $kT \ln 2$ for each bit of information lost [78]. It was recently demonstrated, however, that logic irreversibility does not necessarily implies heat dissipation, provided that the operation is carried out in a thermodynamically reversible manner [79]. On the other hand, reversible logic operations in principle do not generate heat as a result of entropy increase, because they do not erase information. The study of reversible molecular logic systems is interesting for basic science reasons and, in a perspective, also because heat dissipation

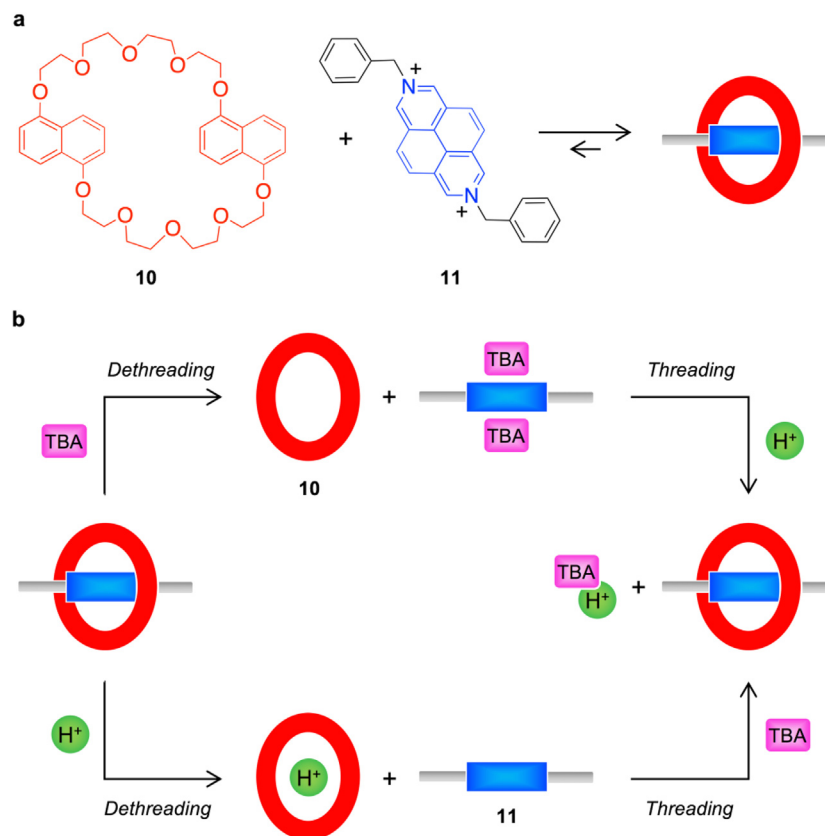


Fig. 8. (a) Structural formulas of ring **10** and axle **11**, and the pseudorotaxane obtained by their self-assembly. (b) Operation scheme of the logic system based on compounds **10** and **11** (TBA = *n*-Bu₃N) [75,77].

is a main issue for the construction of ultra-miniaturized information-processing devices [80].

The present system would become logically reversible if an output signal could enable to distinguish between the $In_1 = In_2 = 0$ (no amine or acid added) and $In_1 = In_2 = 1$ (both amine and acid added) states. Indeed, the triflate anions generated by acid and base neutralization compete with **10** for guest **11**, thereby diminishing the apparent stability of the pseudorotaxane [81]; therefore the emission spectra obtained upon sequential supply of the two inputs do not go back to the initial values upon reset (Out₁, 340 nm and Out₂, 428 nm). Although such an interference compromises the full reversibility of the threading-dethreading process, it allows to distinguish between the $In_1 = In_2 = 0$ and the $In_1 = In_2 = 1$ states. Thus, if the digital output state is established by applying an appropriate threshold to the emission intensity at 340 nm, an OR response can be obtained (see Out₁' in Fig. 9b). Such an operation complements the set of the already discussed XOR and INH functions, and allows reversible logic. Therefore, in this case the *chemical irreversibility* of the transformations caused by the inputs translates into *logic reversibility* of the Boolean operations [76].

Other examples of AND, XOR and INH logic operations performed with switchable pseudorotaxanes have been reported in the literature [82,83].

5. Sequential logic systems

As pointed out in Section 4, the output state of a combinational gate in any given moment of time depends solely on

the input states in the same moment. Hence, combinational devices have no memory. On the contrary, in sequential gates and circuits the output state is determined not only by the current state of the inputs, but also on their previous state [31,32,37–40,44,62,84]. A sequential device can therefore remember its history; in fact, memory circuits are intrinsically sequential.

In logic circuit design, a sequential behavior is achieved by sending the output of a given gate as the input of a preceding gate. Such feedback loops break the unidirectional flow of information that characterizes combinational devices, thereby making input timing relevant for the logic behavior. Chemically, this goal is achieved by taking advantage of the rates of the processes involved in the operation of the gate. Hence, it could be argued that, at the molecular level, while combinational logic can be implemented with equilibrium states (see Section 3), sequential logic also needs to consider - and possibly optimize - kinetics. In this regard, the use of molecular machines can be advantageous because rearrangement rates in these systems encompass a wide range of time scales (from nanoseconds to hours) and can be adjusted by structural design.

Artificial molecular machines that operate according to sequential logic operations are relatively rare [44]. A significant example of a rotaxane-based molecular machine designed to exhibit a memory effect is described in Fig. 10. In rotaxane **12**, chemical (redox) stimuli are used to affect the distribution of the macrocyclic component between the two sites located along the axle (thermodynamic control), while photochemical stimuli set the shuttling rate of the ring between the sites (kinetic control) [85]. As these

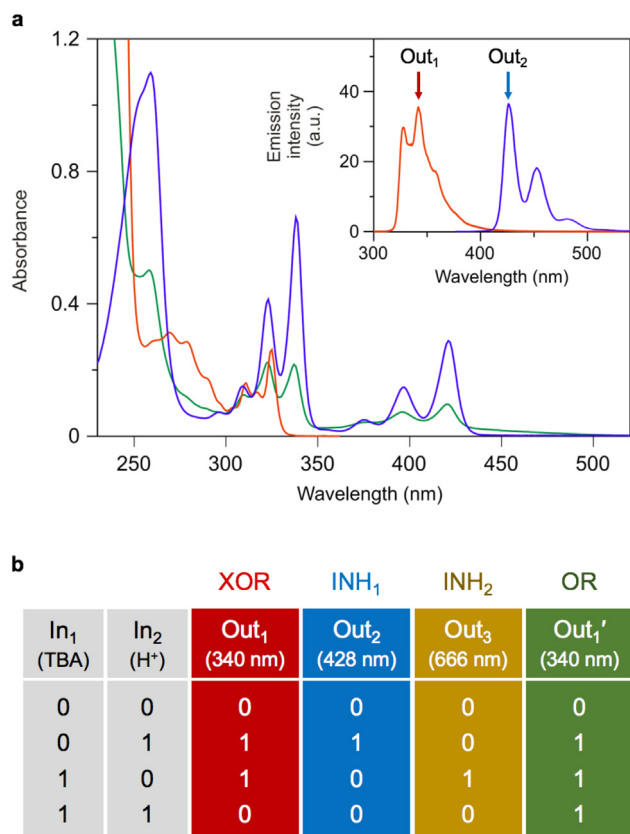


Fig. 9. (a) Absorption and luminescence spectra of **10** (red line) and **11** (blue line) at a concentration of 18 μ M in CH_2Cl_2 - CH_3CN 9:1 at room temperature, together with the absorption spectrum of a 1:1 mixture of **10** and **11** under the same conditions (green line). The inset shows the corresponding luminescence spectra ($\lambda_{\text{ex}} = 264$ nm). (b) Truth table of the logic operations that can be achieved with TBA and acid as the inputs, and luminescence intensity as the output; see the text for details. (For interpretation of the references to colour in this figure legend, the reader is referred to the web version of this article.)

two types of stimuli are mutually orthogonal, they can be considered distinct input signals for the logic device.

Compound **12** (Fig. 10a) is a multicomponent rotaxane based on a well-tested architecture [86] in which the macrocycle is an π -electron-poor cyclobis(paraquat-*p*-phenylene) macrocycle and the axle contains a tetrathiafulvalene (TTF) and a 1,5-dioxynaphthalene (DNP) unit as π -electron-rich recognition sites for the macrocycle. The axle also comprises a photoactive 3,5,3',5'-tetramethylazobenzene (AB) moiety, placed in between the TTF and DNP units, which can be conveniently and reversibly photoswitched between its *trans* and *cis* isomers.

In the initial form of **12**, the ring resides preferentially on the TTF unit (Fig. 10b, top left), because the latter is a better π -electron donor than the DNP unit, as evidenced by the presence of a CT absorption band located at 842 nm. The interaction with the TTF unit can be weakened by chemical oxidation of the TTF to its radical cation ($\text{TTF}^{+\bullet}$) with Fe^{3+} ions: the loss of π -donor-acceptor interactions with the ring and the electrostatic repulsion caused by $\text{TTF}^{+\bullet}$ prompt the shuttling of the macrocycle to the DNP recognition site. Such a process is signaled by the disappearance of both the CT band at 842 nm and the sharp absorption features at around 320 nm, typical of the DNP site not interacting with the macrocyclic ring.

Steady state and time-resolved UV–visible spectroscopic experiments showed that the shuttling process is reversible upon quick chemical reduction of the $\text{TTF}^{+\bullet}$ unit to its neutral state with

decamethylferrocene if the azobenzene-type unit is in the *trans* configuration, whereas if the azobenzene unit is photoisomerized to the *cis* form prior to the $\text{TTF}^{+\bullet} \rightarrow \text{TTF}$ back reduction, the ring remains trapped on the DNP site (Fig. 10b, top right). This behavior can be rationalized considering the larger steric hindrance posed to the ring transit by the *cis*-azobenzene with respect to the *trans* isomer, in line with literature results [87].

A ‘write-lock-erase’ experiment is thus summarized by the cycle shown in Fig. 10b: an oxidation stimulus (In_1) writes information on the rotaxane, which is then locked by UV light irradiation (In_2); after back reduction of the oxidized species, the written data are stored until the azobenzene gate opens by thermal isomerization. Indeed, the data can be read optically in a non-destructive manner at 842 nm and remain stored for a few hours in the dark at room temperature, a significantly longer time compared to thermodynamically controlled molecular switches. Therefore, **12** operates as a bistable memory element under light-triggered kinetic control.

The sequential logic response of **12** to the two inputs can be evidenced by examining the behavior of the rotaxane upon exchanging the order of activation of the inputs (Fig. 11). In a second set of experiments, the azobenzene gate was first closed by UV irradiation, and then the rotaxane was submitted to chemical oxidation. The results showed that the rotaxane in the *cis* configuration becomes oxidized on a much slower time scale than its *trans* form. Such an observation can be interpreted reminding that the movement of the macrocycle away from the TTF unit is kinetically hampered by the presence of the *cis*-azobenzene unit. The oxidation of the TTF unit could be prevented by the presence of the tetracationic ring, entrapped around the TTF site itself, for both thermodynamic (increase of the potential for oxidation) and kinetic (molecular encapsulation, electrostatic repulsion between the positively charged oxidant and macrocycle) reasons.

These results are quite different from those obtained in the ‘write-lock-erase’ cycle experiment (Fig. 10b), confirming that the response of the compound is determined not only by the input states, but also by the order in which these states are changed. Fig. 10b and 11 show that the same input combination ($\text{In}_1 = \text{In}_2 = 1$) can produce a different optical output (transmittance at 842 nm) which is determined by their sequence.

It is interesting to note that the diminished reactivity of *cis*-**12** towards oxidation in comparison with its *trans* counterpart could enable a photochemical write-protection mechanism. Indeed, the photoinduced *trans* \rightarrow *cis* isomerization locks the written information in the previously oxidized rotaxanes (vide supra), while the same photoisomerization slows down oxidation of the non-oxidized species, thus preventing data writing in non-written molecules.

An important family of sequential logic circuits is that of flip-flop devices [57]. In particular, the set-reset (S-R) flip-flop possesses all the basic features of a random access memory (RAM). Its equivalent circuit (Fig. 12a) comprises two NAND (NOT AND), or NOR (NOT OR), gates connected such that the output of a gate is sent back as one input of the other gate. A S-R flip-flop accepts two inputs – S (set) and R (reset) – and has one binary output. The state of the latter is determined by the following rules: S = 1 dictates Out = 1 (thus erasing the output state 0) and preserves it; R = 1 dictates Out = 0 (thus erasing the output state 1) and preserves it. When both S and R are 0, the device maintains its output state (either 0 or 1), whereas the situation in which both S and R are 1 leads to an undefined state of the flip-flop. The truth table depicted in b Fig. 12b summarizes all the possible states of the device, and highlights the fact that the next state of the output depends on its current state.

The behavior of a S-R flip-flop was realized at the molecular level with rotaxane **13** (Fig. 13) [88]. This species is a representa-

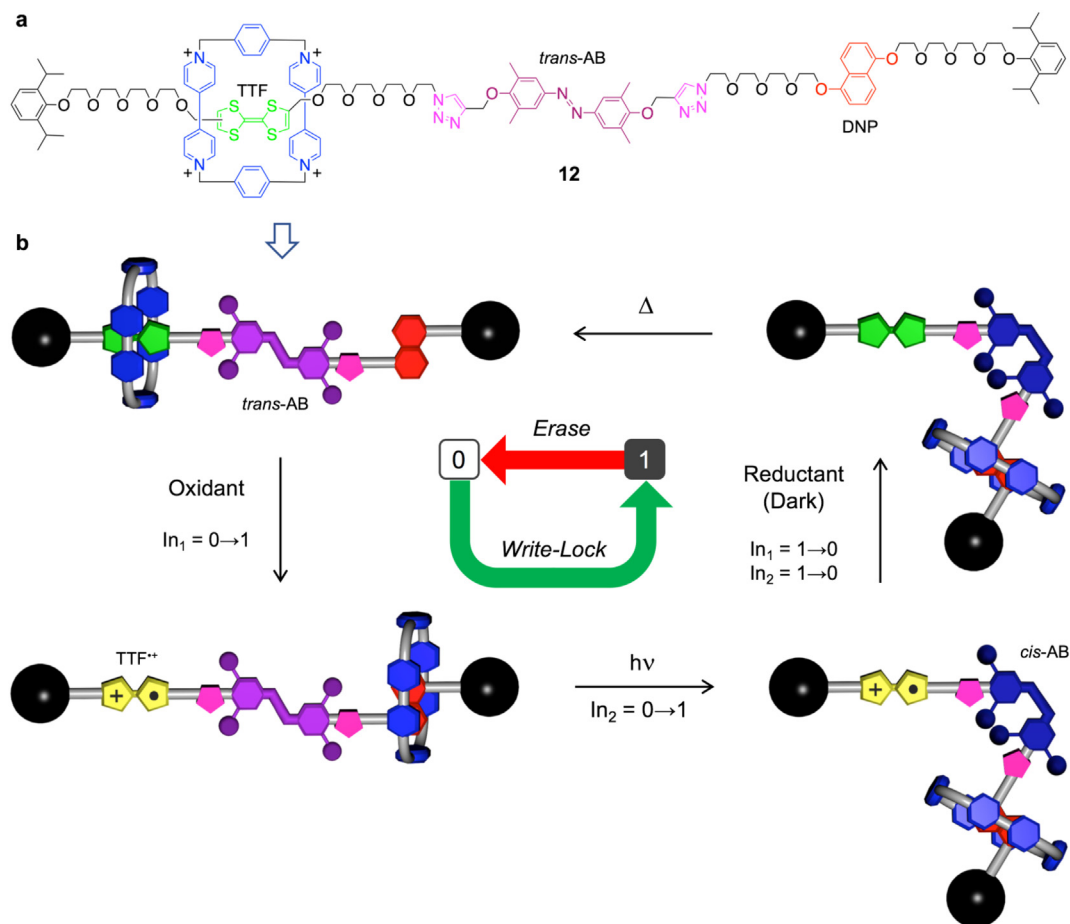


Fig. 10. (a) Structure formula of the rotaxane **12** in its *trans* configuration. (b) Schematic representation of the 'write-lock-erase' memory switching cycle triggered by redox and photochemical stimuli. The diagram should be read counterclockwise starting from the top left corner [85].

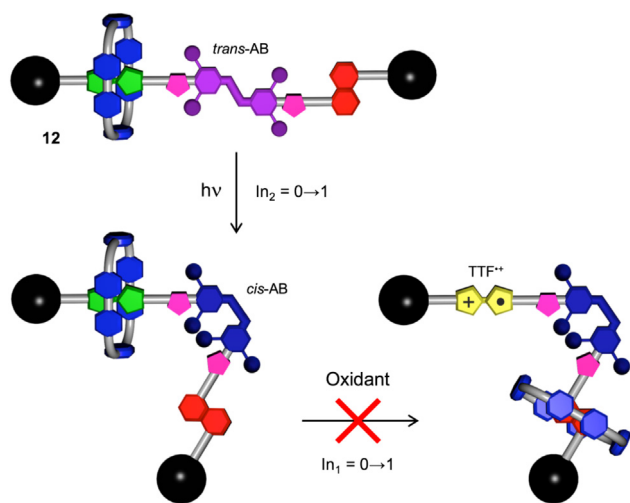


Fig. 11. Schematic representation of the structural changes observed in rotaxane **12** in response to UV irradiation and chemical oxidation, applied in this order.

tive example of an important class of mechanically interlocked compounds, namely, those based on Cu^{I} -polypyridine complexes [15]. It consists of an axle containing one bidentate 2,2'-bipyridine (BPY) ligand and two stoppers, and a macrocyclic ring containing one bidentate phenanthroline (PHEN) and one tridentate terpyridine (TPY) ligand. In the stable structure of **13**, the

Cu^+ ion achieves a tetrahedral coordination to the bidentate ligands in the axle and in the macrocycle (Fig. 13, top left). The electrochemical oxidation of Cu^+ to Cu^{2+} causes the reorganization of the tetracoordinated complex into a five-coordinated one, via the pirouetting of the wheel around the axle. Cyclic voltammetric experiments demonstrated that the process is reversible and were used to investigate the kinetics of the rotation reactions (Fig. 14) [87,89].

The ability of **13** to undergo reversible geometrical reorganization triggered by electrochemical switching between the two different metal oxidation states provides the basis for the bistability necessary to develop a S-R device. An essential feature of the switching in the present case, however, is the hysteresis arising from the nature of the coordination rearrangement about the copper center upon redox stimulation. Such a phenomenon, that determines a large difference between the potential values for oxidation and reduction of the copper ion (Fig. 14), makes it possible to discriminate between the set and reset transitions. The S-R operation (Fig. 12b) requires the definition of three potential values: do nothing ($S = R = 0$), set ($S = 1, R = 0$), and reset ($S = 0, R = 1$). The set potential was fixed as +1.0 V (vs an Ag quasi-reference electrode), a value at which the five-coordinated Cu^{2+} rotaxane complex is the stable species (Out = 1). The reset potential was set at −0.4 V, where the stable species is the tetracoordinated Cu^+ species (Out = 0). The do-nothing potential must be chosen in the bistability region (shaded area in Fig. 14); for example, at +0.2 V the system will be in state 0 (tetracoordinated Cu^+) in the oxidation scan, and in state 1 (five-coordinated Cu^{2+}) in the reduction scan.

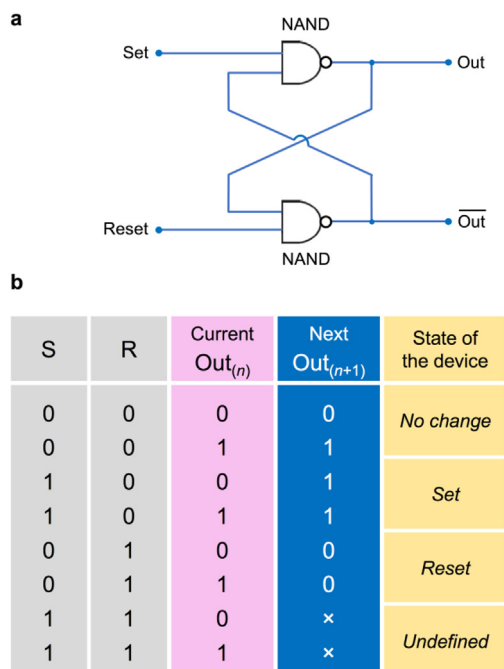


Fig. 12. Logic circuit (a) and truth table (b) of a S-R flip-flop.

The activation of a set input (+1.0 V) switches the output from state 0 to 1 (line 3 in Fig. 12b); however, if the device is already in state 1, the set input has no effect (line 4). If a reset input is applied (−0.40 V), the output turns from 1 to 0 (line 6), while it does not change if it is already in state 0 (line 5). The do-nothing potential (+0.2 V) has no effect on the output state, irrespective of whether the latter is 0 (line 1) or 1 (line 2). The output state can be determined by measuring the electrical current in response to the applied potential input. Rotaxane **13** functions as a memory, because an information bit can be written by activating the S input and remains memorized even when the writing potential is removed, until it is erased by application of an R input. The full chemical reversibility of the redox processes under the condition

employed enables the flip-flop to sustain a large number of switching cycles.

It is worth noting that the same kind of kinetic bistability exhibited by rotaxane **13** was also found for catenanes and rotaxanes based on CT interactions and not containing metal ions (e.g. similar to **12**, Fig. 10) [85]. These compounds were introduced in nanofabricated electrical junctions to make high-density molecule-based electronic memories [90,91]. These outstanding results are not described here because they have been extensively reviewed [1,12,24,25,92]. In general, all these investigations show that large amplitude movements, triggered by externally triggered switching processes, in mechanically interlocked systems can provide the functional elements required to realize the sequential logic operations that are at the basis of information storage.

6. Conclusion

Research of the past three decades in the field of supramolecular chemistry has shown that molecular-based machines can be rationally designed to respond to multiple signals of chemical, electrical and/or optical nature [1–4]. In some cases, these nanoscale mechanical devices have been proven to perform complex combinational and sequential logic operations, such as the sum, subtraction or memorization of binary numbers [31,32]. Mechanically interlocked molecules are appealing platforms for making even more sophisticated computing devices. For example, the design of a chemical Turing machine, based on a rotaxane in which a ring moves catalytically along a polymer thread and prints binary information on it, was hypothesized [93].

From another perspective, the realization of artificial molecular machines and motors that can be activated by specific patterns or sequences of different signals is a fascinating scientific challenge that can now be undertaken. Such a goal is even more attractive if one considers the crucial role of biomolecular machines in living organisms, and the potential of artificial counterparts for innovative technological and medical applications [36,65]. Leaving aside speculations related to the construction of chemical computers and nanorobots, this research is important primarily for its basic science value. Indeed, complex logical and mechanical functionalities arise from a subtle interplay between the thermodynamic and kinetic properties of molecular switching, and can thus be

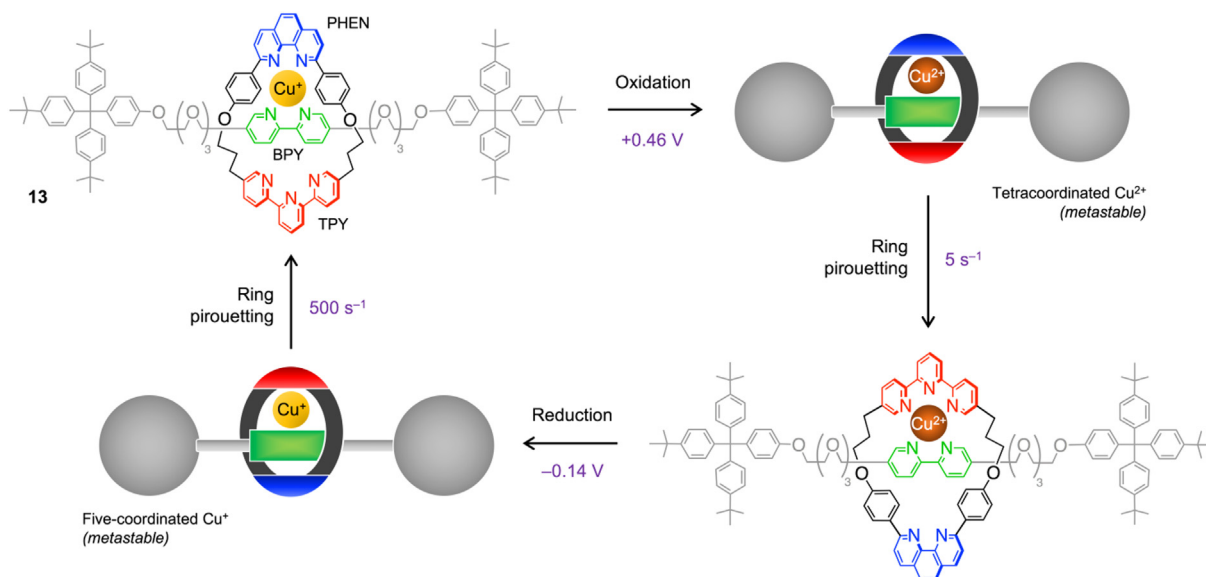


Fig. 13. The electrochemically triggered switching of the redox states in the Cu-rotaxane **13** (horizontal reactions) is followed by complex reorganization (vertical reactions) [88]. Peak potential values for the redox reactions (versus an Ag quasi-reference electrode) and rate constants for ring pirouetting are reported (CH₃CN, room temperature).

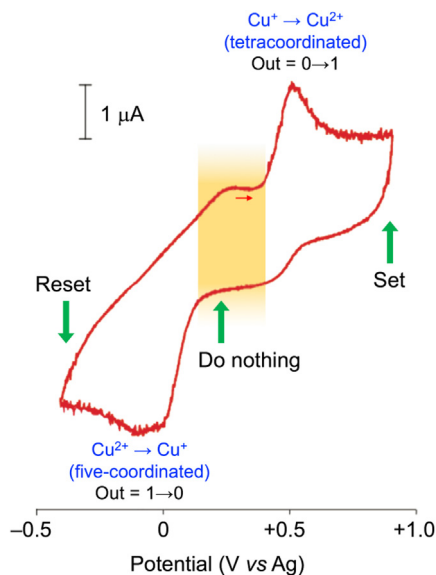


Fig. 14. Cyclic voltammetric scan of rotaxane **13** in acetonitrile at room temperature. The green arrows denote the 'set', 'reset' and 'do nothing' potential values, while the shaded area indicates the region of bistability. Conditions: Pt working electrode, Ag quasi-reference electrode, scan rate 3 V/s. Adapted with permission from Ref. [89]. Copyright 2009 American Chemical Society. (For interpretation of the references to colour in this figure legend, the reader is referred to the web version of this article.)

designed only if these aspects are deeply understood. Moreover, studies such as those reviewed here can contribute to shine light on the intimate molecular mechanisms underlying the operation of living systems [5–7].

A stimulating issue to be investigated is the design of systems that integrate together molecular sensors, logic modules and mechanical actuators. This is a first step forward towards the construction of true molecular robots [54,55]. Other challenges involve the parallel operation of different molecular machines in the same environment [94] and the dynamical programming of the function of the device (that is, reconfiguring it) in response to endogenous or external stimuli [95]. The latter possibility has been demonstrated for basic molecular logic gates [58–61], but it has yet to be explored for molecular machines. Finally, new avenues for multidisciplinary research could arise from the application of concepts that go beyond Boolean logic – such as those of fuzzy logic, neural networks and artificial intelligence [96] – to the molecular movements that take place in multicomponent assemblies.

Declaration of Competing Interest

The authors declare that they have no known competing financial interests or personal relationships that could have appeared to influence the work reported in this paper.

Acknowledgments

This work was supported by the Ministero dell'Università e della Ricerca (PRIN grants 20173L7W8K and 201732PY3X, and FARE grant R16S9XXKX3).

References

- [1] V. Balzani, A. Credi, M. Venturi, *Molecular Devices and Machines - Concepts and Perspectives for the Nanoworld*, Wiley-VCH, Weinheim, 2008.
- [2] J. Wang, *Nanomachines - Fundamentals and Applications*, RSC Publishing, Cambridge, 2012.
- [3] V. Balzani, A. Credi, F.M. Raymo, J.F. Stoddart, *Angew. Chem. Int. Ed.* 39 (2000) 3348–3391.

- [4] S. Erbas-Cakmak, D.A. Leigh, C.T. McTernan, A.L. Nussbaumer, *Chem. Rev.* 115 (2015) 10081–10206.
- [5] M. Schliwa (Ed.), *Molecular Motors*, Wiley-VCH, Weinheim, 2003.
- [6] D.S. Goodsell, *Bionanotechnology: Lessons from Nature*, Wiley-Liss, Hoboken, 2004.
- [7] S. Mann, *Angew. Chem. Int. Ed.* 47 (2008) 5306–5320.
- [8] R.A.L. Jones, *Soft Machines - Nanotechnology and Life*, Oxford University Press, Oxford, 2004.
- [9] L. Zhang, V. Marcos, D.A. Leigh, *Proc. Natl. Acad. Sci. U.S.A.* 115 (2018) 9397–9404.
- [10] J.-M. Lehn, *Angew. Chem. Int. Ed.* 27 (1988) 89–112.
- [11] V. Balzani, A. Credi, M. Venturi, *Chem. Eur. J.* 8 (2002) 5524–5532.
- [12] C. Bruns, J.F. Stoddart, *The Nature of the Mechanical Bond: From Molecules to Machines*, Wiley, Hoboken, 2016.
- [13] S. Kassem, T. van Leeuwen, A.S. Lubbe, M.R. Wilson, B.L. Feringa, D.A. Leigh, *Chem. Soc. Rev.* 46 (2017) 2592–2621.
- [14] K. Ariga, J. Li, J. Fei, Q. Ji, J.P. Hill, *Adv. Mater.* 28 (2016) 1251–1286.
- [15] J.-P. Sauvage, *Angew. Chem. Int. Ed.* 56 (2017) 11080–11093.
- [16] J.F. Stoddart, *Angew. Chem. Int. Ed.* 56 (2017) 11094–11125.
- [17] B.L. Feringa, *Angew. Chem. Int. Ed.* 56 (2017) 11059–11078.
- [18] F. Lancia, A. Ryabchun, N. Katsonis, *Nat. Rev. Chem.* 3 (2019) 536–551.
- [19] D. Dattler, G. Fuks, J. Heiser, E. Moulin, A. Perrot, X. Yao, N. Giuseppone, *Chem. Rev.* 120 (2020) 310–433.
- [20] S. Corra, M. Curcio, M. Baroncini, S. Silvi, A. Credi, *Adv. Mater.* (2020), <https://doi.org/10.1002/adma.201906064>.
- [21] I. Aprahamian, *ACS Cent. Sci.* 6 (2020) 347–358.
- [22] R. Ballardini, V. Balzani, A. Credi, M.T. Gandolfi, M. Venturi, *Acc. Chem. Res.* 34 (2001) 445–455.
- [23] V. Balzani, A. Credi, M. Venturi, *Chem. Eur. J.* 14 (2008) 26–39.
- [24] A. Credi, M. Venturi, V. Balzani, *ChemPhysChem* 11 (2010) 3398–3403.
- [25] Y. Luo, C.P. Collier, J.O. Jeppesen, K.A. Nielsen, E. Delonno, G. Ho, J. Perkins, H.-R. Tseng, T. Yamamoto, J.F. Stoddart, J.R. Heath, *ChemPhysChem* 6 (2002) 519–525.
- [26] S. Silvi, A. Arduini, A. Pochini, A. Secchi, M. Tomasulo, F.M. Raymo, M. Baroncini, A. Credi, *J. Am. Chem. Soc.* 129 (2007) 13378–13379.
- [27] C. Biagini, F. Di Pietri, L. Mandolini, O. Lanzalunga, S. Di Stefano, *Chem. Eur. J.* 24 (2018) 10122–10127.
- [28] G. Ragazzon, C. Schafer, P. Franchi, S. Silvi, B. Colasson, M. Lucarini, A. Credi, *Proc. Natl. Acad. Sci. U.S.A.* 115 (2018) 9385–9390.
- [29] E. Katz, V. Privman, *Chem. Soc. Rev.* 39 (2010) 1835–1857.
- [30] J.R. Gregg, *Ones and Zeros: Understanding Boolean Algebra, Digital Circuits, and the Logic of Sets*, Wiley-IEEE Press, New York, 1998.
- [31] A.P. de Silva, *Molecular Logic-based Computation*, Royal Society of Chemistry, Cambridge, UK, 2013.
- [32] K. Szacilowski, *Infochemistry: Information Processing at the Nanoscale*, Wiley, Chichester, 2012.
- [33] A.P. de Silva, H.Q.N. Gunaratne, C.P. McCoy, *Nature* 364 (1993) 42–44.
- [34] A.P. de Silva, H.Q.N. Gunaratne, T. Gunnlaugsson, A.J.M. Huxley, C.P. McCoy, J.T. Rademacher, T.E. Rice, *Chem. Rev.* 97 (1997) 1515–1566.
- [35] F.M. Raymo, *Adv. Mater.* 14 (2002) 401–414.
- [36] A.P. de Silva, S. Uchiyama, *Nat. Nanotechnol.* 2 (2007) 399–410.
- [37] K. Szacilowski, *Chem. Rev.* 108 (2008) 3481–3548.
- [38] M. Amelina, L. Zou, A. Credi, *Coord. Chem. Rev.* 254 (2010) 2267–2280.
- [39] J. Andreasson, U. Pischel, *Chem. Soc. Rev.* 44 (2015) 1053–1069.
- [40] S. Erbas-Cakmak, S. Kolenen, A.C. Sedgwick, T. Gunnlaugsson, T.D. James, J. Yoon, E.U. Akkaya, *Chem. Soc. Rev.* 47 (2018) 2228–2248.
- [41] B.L. Feringa, W.R. Browne (Eds.), *Molecular Switches*, Second Edition, Wiley-VCH, Weinheim, 2011.
- [42] J.D. Harris, M.J. Moran, I. Aprahamian, *Proc. Natl. Acad. Sci. U.S.A.* 115 (2018) 9414–9422.
- [43] R. Ballardini, P. Ceroni, A. Credi, M.T. Gandolfi, M. Maestri, M. Semeraro, M. Venturi, V. Balzani, *Adv. Funct. Mater.* 17 (2007) 740–750.
- [44] T. Avellini, M. Baroncini, G. Ragazzon, S. Silvi, M. Venturi, A. Credi, *Isr. J. Chem.* 54 (2014) 553–567.
- [45] N.C. Seeman, A.M. Belcher, *Proc. Natl. Acad. Sci. U.S.A.* 99 (2002) 6451–6455.
- [46] P.W. Rothmund, *Nature* 440 (2006) 297–302.
- [47] D.Y. Zhang, G. Seeling, *Nat. Chem.* 2 (2011) 103–113.
- [48] W. Fuang, C.-H. Lu, I. Willner, *Chem. Rev.* 114 (2014) 2881–2941.
- [49] C.-H. Lu, A. Ceconello, J. Elbaz, A. Credi, I. Willner, *Nano Lett.* 3 (2013) 2303–2308.
- [50] H.Z. Gu, J. Chao, S.J. Xiao, N.C. Seeman, *Nature* 465 (2010) 202–205.
- [51] T. Li, F. Lohmann, M. Famulok, *Nat. Commun.* 5 (2014) 4940.
- [52] T. Nakama, Y. Takezawa, D. Sasaki, M. Shionoya, *J. Am. Chem. Soc.* 142 (2020) 10153–10162.
- [53] S.M. Douglas, I. Bachelet, G.M. Church, *Science* 335 (2012) 831–834.
- [54] M. Hagiya, A. Konagaya, S. Kobayashi, H. Sato, S. Murata, *Acc. Chem. Res.* 47 (2014) 1681–1690.
- [55] N.C. Seeman, H.F. Sleiman, *Nat. Rev. Mater.* 3 (2018) 17068.
- [56] D.M. Kolpashchikov, *Acc. Chem. Res.* 52 (2019) 1949–1956.
- [57] P.L. Gentili, *ChemPhysChem* 12 (2011) 739–745.
- [58] A.A. Kumar, *Fundamentals of Digital Circuits*, fourth ed., PHI Learning, Delhi, 2016.
- [59] D. Margulies, G. Melman, A. Shanzer, *Nat. Mater.* 4 (2005) 768–771.
- [60] M. Amelina, M. Baroncini, A. Credi, *Angew. Chem. Int. Ed.* 47 (2008) 6240–6243.
- [61] P. Ceroni, G. Bergamini, V. Balzani, *Angew. Chem. Int. Ed.* 48 (2009) 8516–8518.

- [62] A.P. de Silva, N.D. McClenaghan, *Chem. Eur. J.* **8** (2002) 4935–4945.
- [63] A. Credi, *Angew. Chem. Int. Ed.* **46** (2007) 5472–5476.
- [64] P.R. Ashton, V. Baldoni, V. Balzani, A. Credi, H.D.A. Hoffmann, M.V. Martinez-Diaz, F.M. Raymo, J.F. Stoddart, M. Venturi, *Chem. Eur. J.* **7** (2001) 3482–3493.
- [65] S. Muramatsu, K. Kinbara, H. Taguchi, N. Ishii, T. Aida, *J. Am. Chem. Soc.* **128** (2006) 3764–3769.
- [66] A. Credi, Potential applications of molecular logic, in: J.-P. Sauvage, P. Gaspard (Eds.), *From Non-Covalent Assemblies to Molecular Machines*, Wiley-VCH, Weinheim, 2010.
- [67] P.K. Biswas, S. Saha, S. Gaikwad, M. Schmittle, *J. Am. Chem. Soc.* **142** (2020) 7889–7897.
- [68] P.K. Biswas, S. Saha, T. Paululat, M. Schmittle, *J. Am. Chem. Soc.* **140** (2018) 9038–9041.
- [69] S. Angelos, Y.-W. Yang, N.M. Khashab, J.F. Stoddart, J.I. Zink, *J. Am. Chem. Soc.* **131** (2009) 11344–11346.
- [70] S. Saha, K.-C.-F. Leung, T.D. Nguyen, J.F. Stoddart, J.I. Zink, *Adv. Funct. Mater.* **17** (2007) 685–693.
- [71] S. Angelos, E. Choi, F. Vögtle, L. De Cola, J.I. Zink, *J. Phys. Chem. C* **111** (2007) 6589–6592.
- [72] H. Li, J.-N. Zhang, W. Zhou, H. Zhang, Q. Zhang, D.-H. Qu, H. Tian, *Org. Lett.* **15** (2013) 3070–3073.
- [73] J. Cao, X. Ma, M. Min, T. Cao, S. Wu, H. Tian, Related example of a [1]pseudorotaxane that behaves as a INH gate, *Chem. Commun.* **50** (2014) 3224–3226.
- [74] D.A. Leigh, M.A.F. Morales, E.M. Pérez, J.K.Y. Wong, C.G. Saiz, A.M.Z. Slawin, A.J. Carmichael, D.M. Haddleton, A.M. Brouwer, W.J. Buma, G.W.H. Wurpel, S. Leon, F. Zerbetto, *Angew. Chem. Int. Ed.* **44** (2005) 3062–3067.
- [75] V. Balzani, A. Credi, S.J. Langford, J.F. Stoddart, *J. Am. Chem. Soc.* **119** (1997) 2679–2681.
- [76] P. Ball, *Nature* **406** (2000) 118–120.
- [77] M. Semeraro, A. Credi, *J. Phys. Chem. C* **114** (2010) 3209–3214.
- [78] R. Landauer, *IBM J. Res. Dev.* **5** (1961) 183–191.
- [79] M. López-Suárez, I. Neri, L. Gammaitoni, *Nat. Commun.* **7** (2016) 12068.
- [80] A. Béruit, A. Arakelyan, A. Petrosyan, S. Ciliberto, R. Dillenschneider, E. Lutz, *Nature* **483** (2012) 187–189.
- [81] M. Clemente-León, C. Pasquini, V. Hebbe-Viton, J. Lacour, A. Dalla Cort, A. Credi, *Eur. J. Org. Chem.* (2006) 105–112.
- [82] M. Asakawa, P.R. Ashton, V. Balzani, A. Credi, G. Mattersteig, O.A. Matthews, M. Montalti, N. Spencer, J.F. Stoddart, M. Venturi, *Chem. Eur. J.* **3** (1997) 1992–1996.
- [83] C. Gao, S. Silvi, X. Ma, H. Tian, M. Venturi, A. Credi, *Chem. Commun.* **48** (2012) 7577–7579.
- [84] G. de Ruiter, M.E. van der Boom, *J. Mater. Chem.* **21** (2011) 17575–17581.
- [85] T. Avellini, H. Li, A. Coskun, G. Barin, A. Trabolsi, A.N. Basuray, S.K. Dey, A. Credi, S. Silvi, J.F. Stoddart, M. Venturi, *Angew. Chem. Int. Ed.* **51** (2012) 1611–1615.
- [86] J.W. Choi, A.H. Flood, D.W. Steuerman, S. Nygaard, A.B. Braunschweig, N.N.P. Moonen, B.W. Laursen, Y. Luo, E. Delonno, A.J. Peters, J.O. Jeppesen, K. Xu, J.F. Stoddart, J.R. Heath, *Chem. Eur. J.* **12** (2006) 261–279.
- [87] M. Baroncini, S. Silvi, M. Venturi, A. Credi, *Chem. Eur. J.* **16** (2010) 11580–11587.
- [88] G. Periyasamy, J.-P. Collin, J.-P. Sauvage, R.D. Levine, F. Remacle, *Chem. Eur. J.* **15** (2009) 1310–1314.
- [89] G. Periyasamy, A. Sour, J.-P. Collin, J.-P. Sauvage, F. Remacle, *J. Phys. Chem. B* **113** (2009) 6219–6229.
- [90] C.P. Collier, G. Mattersteig, E.W. Wong, Y. Luo, K. Beverly, J. Sampaio, F.M. Raymo, J.F. Stoddart, J.R. Heath, *Science* **289** (2000) 1172–1175.
- [91] J.E. Green, J.W. Choi, A. Boukai, Y. Bunimovich, E. Johnston-Halperin, E. Delonno, Y. Luo, B.A. Sherif, K. Xu, Y.S. Shin, H.-R. Tseng, J.F. Stoddart, J.R. Heath, *Nature* **445** (2007) 414–417.
- [92] S. Silvi, M. Venturi, A. Credi, *J. Mater. Chem.* **19** (2009) 2279–2294.
- [93] S. Varghese, J.A.A.W. Elemans, A.E. Rowan, R.J.M. Nolte, *Chem. Sci.* **6** (2015) 6050–6058.
- [94] M. Ueda, S. Terazawa, Y. Deguchi, M. Kimura, N. Matsubara, S. Miyagawa, T. Kawasaki, Y. Tokunaga, *Chem. Asian J.* **11** (2016) 2291–2300.
- [95] L. Yue, S. Wang, A. Cecconello, J.-M. Lehn, I. Willner, *ACS Nano* **11** (2017) 12027–12036.
- [96] P.L. Gentili, *Molecules* **23** (2018) 2074–2091.